Int. J. Heat Mass Transfer. Vol. 36, No. 9, pp. 2403–2415, 1993
Printed in Great Britain

0017-9310/93 $6.00 + 0.00

Diffusion controlled evaporation of a multicomponent droplet: theoretical studies on the importance of variable liquid properties

R. KNEER, M. SCHNEIDER, B. NOLL and S. WITTIG
Lehrstuhl und Institut für Thermische Strömungsmaschinen, Universität Karlsruhe (T.H.), Kaiserstr. 12, W-7500 Karlsruhe, Germany

(*Received* 17 *December* 1991 *and in final form* 8 *July* 1992)

Abstract—A well-known multicomponent droplet vaporization model, the Diffusion Limit Model, has been extended to account for property variations in the liquid phase. The model has been tested for typical conditions of modern gas turbine combustors. The results for a hexane/tetradecane droplet show that the temperature- and concentration-dependence of the liquid properties affect the vaporization process, especially with regard to a reduced diffusional resistance. Additionally, remarkable variations of the refractive index are observed yielding helpful information for the estimation of errors in optical particle sizing techniques. Regarding comprehensive spray calculations, the use of the constant property formulation is recommended with improved reference values based on variable property calculations.

INTRODUCTION

General aspects

LIQUID fuel combustion processes in gas turbine combustors are mainly influenced by the mixing of fuel and air (cf. Wittig *et al.* [1, 2]). Especially, the fuel evaporation behavior is of importance, which is determined by the chemical and physical fuel properties. Typical hydrocarbon fuels consist of several hundreds or even thousands of components and show a wide boiling range due to volatility differentials, in contrast to a single component liquid marked by a distinct boiling point. Therefore, realistic spray evaporation modeling should account for the multicomponent nature of the fuel. In the present paper, the simplest case (where both volatility differentials and the mass diffusion within the fuel droplets become important) is represented by a bicomponent mixture.

In the vaporization literature several multicomponent droplet models have been described accounting for temperature and concentration variations within the droplet, which is considered to be a fundamental requirement to obtain results with acceptable accuracy. However, multicomponent droplet models reported so far are based on constant property formulations. Results show that large temperature and concentration gradients develop within a droplet during the transient vaporization. Since the thermophysical properties of the liquid such as the diffusion coefficient and thermal conductivity are dependent on temperature and composition, the question arises as to how these quantities are affected and to what extent the vaporization process itself is influenced.

In the present study, a multicomponent droplet vaporization model is developed accounting for the variations of thermophysical liquid properties. The objective is to determine the degree of complexity necessary for use with a multicomponent spray evaporation model. The present model is based on earlier contributions of Landis and Mills [3] and Law [4], who have shown that liquid diffusion can be the rate controlling process for the entire droplet lifetime.

Literature review

In recent years, considerable progress has been made in the development of single component vaporization models. The first steps in droplet modeling were marked by the exclusion of the internal heat transport process (see the reviews of Sirignano [5, 6], Faeth [7] and Law [8]). Present droplet vaporization modeling enables the computation of both the flow field around the droplet and the internal fluid motion. The detailed description of the internal transport is time-consuming in computation and thus allows the consideration of isolated droplets.

Recent studies were carried out by Dwyer and Sanders [9, 10], Haywood *et al.* [11], Haywood and Renksizbulut [12], Oliver and Chung [13], Huang and Ayyaswamy [14], as well as Sadhal and Ayyaswamy [15]. These calculations were conducted either for a steady case [15] or they neglected the variation of gas phase properties (see Dwyer and Sanders [9, 10]), the latter being extremely important to the heat and mass transfer. For that reason, the results of Huang and Ayyaswamy [14] and Haywood and co-workers [11, 12] seem to be the most reasonable, although Huang and Ayyaswamy [14] identify the incorrect formulation of the momentum equation in refs. [11, 12].

In using the above mentioned 'internal motion

NOMENCLATURE

a	thermal diffusivity, $\lambda/\rho c_p$
c_D	drag coefficient
c_p	specific heat [J kg^{-1} K^{-1}]
d_d	droplet diameter [m]
D	diffusion coefficient [m^2 s^{-1}]
L	enthalpy of vaporization [J kg^{-1}]
Le	Lewis number, $\lambda/\rho c_p D$
M	molar weight [kg kmol^{-1}]
m	mass [kg]
$\dot{m}$	vaporization rate [kg s^{-1}]
n	refractive index
Pe	Peclet number, $K_s(t)/D_l$
Pr	Prandtl number, ν/a
p_V	vapor pressure [N m^{-2}]
$\dot{Q}_{Heat}$	amount of $\dot{Q}_{Net}$ transferred into the droplet [W]
$\dot{Q}_{Net}$	total heat flow rate transferred towards the droplet [W]
$\dot{Q}_{Vap}$	amount of $\dot{Q}_{Net}$ necessary to vaporize the fraction $\dot{m}$ [W]
R_m	molar refractivity [m^3 kmol^{-1}]
r	radial coordinate [m]
r_d	instantaneous droplet radius [m]
Sc	Schmidt number, ν/D
t	time [s]
T	temperature [K]
u	velocity [m s^{-1}]
V_m	mixture molar volume [kg kmol^{-1}]
X	molar fraction
Y	mass fraction.

Greek symbols

α	heat transfer coefficient [W m^{-2} K^{-1}]
ε_i	partial vaporization rate, $\dot{m}_i/\dot{m}$
ζ	non-dimensional actual droplet radius, $r_d/r_{d,0}$
λ	thermal conductivity [W m^{-1} K^{-1}], wavelength [m]
ν	frequency [s^{-1}], kinematic viscosity [m^2 s^{-1}]
ρ	density [kg m^{-3}]
ω	non-dimensional radial coordinate, r/r_d.

Subscripts

c	critical value
d	droplet
g	gas phase
i	component
ref	reference value
s	surface
V	vapor
0	initial value
∞	free-stream condition.

droplet models' the drag coefficient c_D is obtained directly during the calculation. Therefore, these models are also used for the testing of existing c_D-correlations. Based on their calculations Renksizbulut and co-workers [16, 17] as well as Chiang *et al.* (cited in ref. [18]) suggest the use of c_D-correlations corrected with respect to surface blowing. However, these correlations are experimentally verified only for a range of relatively low mass transfer numbers ($B_m < 3$). As a result of the complexity of these models they cannot be applied to comprehensive spray calculations. However, results from these models can serve to develop simplified models, as suggested by Renksizbulut and Haywood [17].

The vortex model presented by Prakash and Sirignano [19, 20], which approximates the internal circulation by an analytical solution of Hill [21], is able to calculate the vaporization of a multicomponent droplet (see Lara-Urbaneja and Sirignano [22] and Tong and Sirignano [23]). The importance of the variation of the gas phase properties is emphasized by Abramzon and Sirignano [24] who conducted calculations with finite and infinite heat conductivity within the droplet. The effect of gas phase property variations is subsequently taken into consideration in a simplified vortex model, where, similar to the approach of Talley and Yao [25], the effect of internal convection is included by modifying the transport properties of a simpler model.

The work of Aggarwal [26, 27] showed that the transient heating of the liquid may have a significant influence on the mass diffusion process and therefore on the evaporation behavior. If internal convection is also considered, using a vortex model, the mass transport is enhanced only along the streamlines. Therefore, the most important result of [26, 27] is the recommendation of the Diffusion Limit Model emphasizing that the most essential feature of radial mass transport inside the droplet is the diffusion of the liquid components. Moreover, in the case of multicomponent droplet vaporization the effect of internal convection seems to be of less importance compared to single component vaporization.

Both the work of Aggarwal and the results of Gauthier *et al.* [28] and Bergeron and Hallett [29] show that in case of spray calculation the consideration of multicomponent fuel behavior can be essential. An additional effect may be observed if the boiling temperatures of the droplet components are extremely different. In this case microexplosions may occur (see Presser *et al.* [30], Lasheras *et al.* [31], Law [4] and Wang *et al.* [32]).

In the present study a multicomponent droplet model is described, which accounts for the variations of thermophysical liquid and gas phase properties. Thus, the conditions leading to microexplosion may be identified and checked. The modifications introduced into the governing equations and their influence

on the basic features of multicomponent droplet evaporation will be explained in the following Sections.

ANALYSIS

Gas phase

The present model describes the physical behavior of an isolated multicomponent droplet in a stagnant hot environment. Spherical symmetry reduces the problem to a transient process of one-dimensional nature. All physical properties of both liquid and gas phase are treated as variable properties. These properties depend on the temperature and composition and are determined by using the presently available correlations from literature listed in Table 1.

The gas phase is assumed to be quasi-steady applying an integral formulation of the governing equations for a stagnant environment (Hubbard *et al.* [33] and Abramzon and Sirignano [24, 34]). The droplet surface is assumed to be impermeable with respect to the ambient air, which leads to a one-way diffusion of the fuel vapor, the so-called Stefan flow.

To study the evaporation behavior in a non-stagnant environment, convective correction factors for heat and mass transfer are employed, as suggested by Frössling [35]. To account for the effect of the Stefan flow in the convective case, the film theory model of Abramzon and Sirignano [24, 34] is used.

Liquid phase

As mentioned above, the evaporation of a multicomponent droplet in a nonreactive hot environment is considered. Neglecting the internal circulation, only heat conduction and mass diffusion govern the heat and mass transport process. The corresponding equations are derived for a spherical symmetric frame of reference and depend on the treatment of the thermophysical properties. Assuming these properties to be constants, the standard formulation of the liquid phase equations is obtained, which can be found in the papers of Landis and Mills [3], Law [4], Makino and Law [36] and Abramzon and Sirignano [34]. A more accurate formulation of the problem can be derived taking the temperature- and concentration-dependence of the liquid properties into account

$$\frac{\partial T_d}{\partial t} = a_d\left[\frac{\partial^2 T_d}{\partial r^2} + \left(\frac{2}{r} + \frac{1}{\lambda_d}\frac{\partial \lambda_d}{\partial r}\right)\frac{\partial T_d}{\partial r}\right] \tag{1}$$

and

$$\frac{\partial Y_{i,d}}{\partial t} = D_{AB}\left[\frac{\partial^2 Y_{i,d}}{\partial r^2} + \left(\frac{2}{r} + \frac{1}{\rho_d}\frac{\partial \rho_d}{\partial r} + \frac{1}{D_{AB}}\frac{\partial D_{AB}}{\partial r}\right)\frac{\partial Y_{i,d}}{\partial r}\right] - Y_{i,d}\frac{1}{\rho_d}\frac{\partial \rho_d}{\partial t} \tag{2}$$

Table 1. Thermophysical property correlations†

Property	Method	Mixing-rule
Liquid properties		
Density	mod. Rackett (Spencer *et al.* [40, 41])	Chueh-Prausnitz (Daubert [42])
Specific heat	Watson and Nelson‡ [43]	
Thermal conductivity	Latini (in [44])	Baroncini (in [44])
Binary diffusion coefficient	Lusis, Ratcliff/Vignes	
Viscosity	Van Velzen, Cardozo and Langenkamp	
Gas phase properties		
Density	Ideal gas Compressibility factor (Lee and Kesler [45]) Crit. properties (Prausnitz and Gunn (cited in [46]))	
Specific heat§	Reid *et al.* [39]	
Viscosity§	Thodos *et al.*	Chapman-Enskog/Wilke
Thermal conductivity§	Roy, Thodos	Wassiljewa/Lindsay, Bromley
Diffusion coefficient	Binary: Fuller, Schettler and Giddings Mixture: Bird *et al.* [47]	

† Where no explicit sources are given the formulations have been taken out of the standard book of Reid *et al.* [39]. The enthalpy of vaporization and the vapor pressure determining the phase change of the mixture components are calculated with Watson's [48] formula and the Cox–Antoine equation (see ref. [39]). The coefficients of the Cox–Antoine equation have been fitted using literature values of the vapor pressure (Vargaftik [49]).

‡ Molar-averaged boiling temperature employed.

§ Without pressure correction. In the range investigated these properties are only weak functions of pressure.

where the additional terms due to variable property calculation are underlined.

The solution of equations (1) and (2) depends on the initial conditions for the temperature and composition and on the formulation of appropriate boundary conditions. The boundary conditions result from symmetry at the origin and from the energy and mass balance at the droplet surface,

$r = 0$:

$$\frac{\partial T_d}{\partial r} = 0; \quad \frac{\partial Y_{i,d}}{\partial r} = 0 \tag{3}$$

$r = r_d(t)$:

$$4\pi r_d^2 \lambda_d \frac{\partial T}{\partial r} = \dot{Q}_{Net} - \dot{Q}_{Vap} \tag{4}$$

$$\rho_d D_{AB} \frac{\partial Y_{i,d}}{\partial r} = \frac{\dot{m}}{4\pi r_d^2}(Y_{i,d,s} - \varepsilon_i) \tag{5}$$

where

$$\dot{Q}_{Net} = 4\pi r_d^2 \alpha (T_{g,\infty} - T_{g,s})$$

and

$$\dot{Q}_{Vap} = \dot{m} \sum_{i=1}^{n} \varepsilon_i L_i.$$

$\dot{Q}_{Net}$ represents the total heat flow rate transferred towards the droplet, whereas $\dot{Q}_{Vap}$ is the part of the total heat flow rate necessary for the phase change of the instantaneous evaporating mass.

The actual droplet diameter used in the boundary conditions is obtained from a liquid phase mass balance, which leads after differentiation to the final form

$$\frac{dr_d}{dt} = -\frac{1}{\rho_d(r_d, t) r_d^2}\left(\frac{\dot{m}}{4\pi} + \int_0^{r_d(t)} \frac{\partial \rho_d}{\partial t} r^2 \, dr\right). \tag{6}$$

Without rearrangement of the governing equations, the droplet diameter reduction during the vaporization process would cause considerable difficulties with regard to the numerical grid. With reference to Landis and Mills [3] a nondimensionalized spatial coordinate,

$$\omega = \frac{r}{r_d(t)} \tag{7}$$

and an instantaneous droplet diameter,

$$\zeta = \frac{r_d}{r_{d,0}} \tag{8}$$

are introduced to fix the moving boundary. Then, the governing equations can be transformed to

$$\frac{r_{d,0}^2}{a_d}\zeta^2 \frac{\partial T_d}{\partial t} = \frac{\partial^2 T_d}{\partial \omega^2} + \left(\frac{2}{\omega} + \underline{\frac{1}{\lambda_d}\frac{\partial \lambda_d}{\partial \omega}} + \frac{r_{d,0}^2}{a_d}\omega\zeta\frac{d\zeta}{dt}\right)\frac{\partial T_d}{\partial \omega} \tag{9}$$

$$\frac{r_{d,0}^2}{D_{AB}}\zeta^2 \frac{\partial Y_{i,d}}{\partial t} = \frac{\partial^2 Y_{i,d}}{\partial \omega^2} + \left(\frac{2}{\omega} + \underline{\frac{1}{\rho_d}\frac{\partial \rho_d}{\partial \omega}} + \underline{\frac{1}{D_{AB}}\frac{\partial D_{AB}}{\partial \omega}} + \frac{r_{d,0}^2}{D_{AB}}\omega\zeta\frac{d\zeta}{dt}\right)\frac{\partial Y_{i,d}}{\partial \omega} - \underline{\frac{r_{d,0}^2}{D_{AB}}\frac{Y_{i,d}}{\rho_d}\left(\zeta^2\frac{\partial \rho_d}{\partial t} - \omega\zeta\frac{d\zeta}{dt}\frac{\partial \rho_d}{\partial \omega}\right)}. \tag{10}$$

The additional terms resulting from the variable property formulation are again underlined. The time derivative of the droplet diameter is transformed to

$$\frac{d\zeta}{dt} = -\frac{1}{r_{d,0}} \frac{\dfrac{\dot{m}}{4\pi r_d^2} + r_d \displaystyle\int_0^1 \frac{\partial \rho_d}{\partial t}\omega^2 \, d\omega}{\rho_d(\omega = 1, t) - \displaystyle\int_0^1 \frac{\partial \rho_d}{\partial \omega}\omega^3 \, d\omega} \tag{11}$$

and the boundary conditions are rearranged to

$\omega = 0$:

$$\frac{\partial T_d}{\partial \omega} = 0; \quad \frac{\partial Y_{i,d}}{\partial \omega} = 0 \tag{12}$$

$\omega = 1$:

$$\frac{\partial T}{\partial \omega} = \frac{r_d}{\lambda_d}\left(\alpha(T_{g,\infty} - T_{g,s}) - \frac{\dot{m}}{4\pi r_d^2}\sum_{i=1}^{n}\varepsilon_i L_i\right) \tag{13}$$

$$\frac{\partial Y_{i,d}}{\partial \omega} = \frac{\dot{m}}{4\pi \rho_d D_{AB} r_d}(Y_{i,d,s} - \varepsilon_i). \tag{14}$$

Solution procedure

(a) *Coupling of gas and liquid phase.* The gas and the liquid phase are related by the phase change, which takes place at the droplet surface. Assuming ideal liquid and ideal gas phase behavior (activity and fugacity coefficients equal to one) the equilibrium condition at the liquid–gas interface is determined using Raoult's law. Thus, the set of equations is closed and the solution procedure can be described as follows:

The equilibrium condition yields the molar fractions of the species in the gas phase, which are used to calculate the total and partial vaporization rates and the heat transfer coefficient. These are necessary for the evaluation of the boundary conditions at the droplet surface, equations (13) and (14). Thus, the boundary conditions at the droplet surface can be determined and the numerical solution of the partial differential equations, equations (9) and (10), governing the liquid phase behavior is obtained as described in the next section.

(b) *Numerical solution procedure.* The temperature and concentration distributions within the droplet are discretized using the Crank–Nicolson scheme. The resulting set of algebraic equations is solved by a suitable direct solution procedure. The time steps are controlled by two different criteria to avoid oscillations of the solution:

(i) the surface temperature rise is limited by a maximum value. This is important during the early stage of the vaporization process when the droplet surface heats up rapidly;

(ii) the diameter regression towards the final stage of the droplet lifetime is restricted to a maximum value allowing the calculation to proceed towards very small droplet diameters (usually 2% of the initial diameter).

A uniform mesh for the nondimensional spatial (radial) coordinate ω of 100 grid points is employed in all the calculations presented here. However, detailed studies revealed that the number of grid points can be reduced to 20 resulting only in minor deviations of the solution. The differential equations governing the droplet motion are integrated by means of a predictor–corrector method (see Hindmarsh [37]). In order to couple the solutions of droplet vaporization and droplet motion, the time steps of both solutions are adapted by controlling the changes in droplet mass and Reynolds number.

RESULTS AND DISCUSSION

The combination of hexane/tetradecane, which will be discussed here, was found to represent the most interesting case mainly in two aspects. First, this combination can be considered as a simple model of a wide-cut aircraft fuel and secondly, the characteristics of multicomponent evaporation behavior will be emphasized most, as expected. The gas temperature levels selected are typical for gas turbine combustors, where evaporating droplets experience moderate gas temperatures in the prevaporization/premixing zones. Higher-range temperatures are encountered in the primary zone of typical gas turbine combustors. Emphasizing the basic phenomena of multicomponent droplet evaporation the major part of the results is related to the stagnant droplet case, with no relative velocity between the droplet and the surrounding gas. Gas phase convection is taken into account for one test case.

It should be noted that the calculation requires the inclusion of the limit of superheat [4] to detect microexplosions within the liquid bulk due to overheating of the more volatile component. However, in the presented calculations the limit of superheat was not reached in any case, indicating that within the mixtures investigated no microexplosions would take place.

Results are presented for a hexane/tetradecane droplet with an initial mass ratio of one and a uniform internal temperature distribution. The initial droplet diameter is $d_0 = 100$ μm. The results cover calculations for both moderate and high gas temperatures, $T_\infty = 800$ K and $T_\infty = 2000$ K, respectively, at a pressure level of $p_\infty = 10$ bar excluding the combustion process. The subsequent discussion will cover the main features of diffusion-controlled vaporization first. Then, the view is focused on the variation of the properties themselves, particularly with respect to optical measuring techniques. In a third part the effects on the vaporization process due to variable properties are analyzed with regard to constant property calculations.

Diffusion-controlled vaporization

The spatial and time-dependent distribution of droplet temperature and concentration is shown in Figs. 1 and 2 to illustrate the internal heating and diffusion process as the vaporization proceeds.

Figure 1 clearly shows that the moderate gas temperature case yields only minor internal temperature gradients, whereas at high gas temperature levels the temperature distribution reveals large gradients, especially during the first half of the droplet lifetime. Development and magnitude of internal temperature gradients depend basically both on the temperature difference between droplet surface and ambient gas phase and on the liquid thermal diffusivity. The final temperature levels are nearly identical for both ambient temperature levels considered. This is due to identical boiling temperatures, which depend on the ambient pressure.

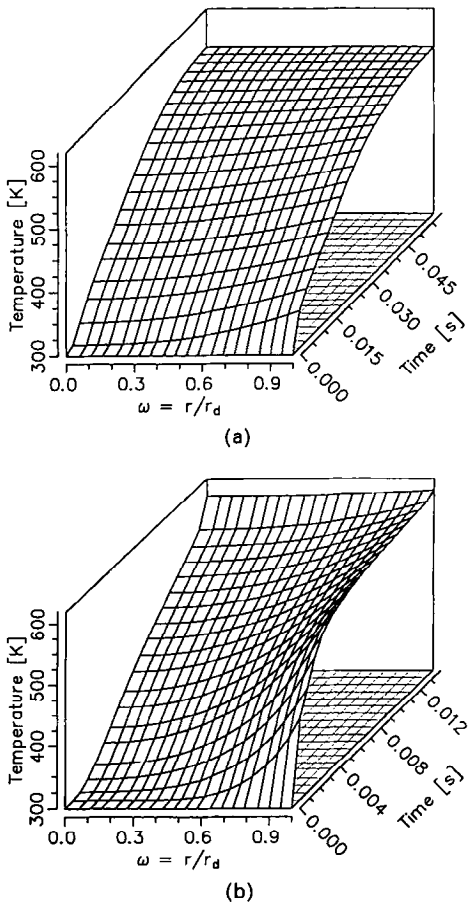

FIG. 1. Temperature distribution within a hexane/tetradecane droplet. Initial mass ratio: $m_{\mathrm{Hex}}/m_{\mathrm{Tet}} = 1$. Ambient pressure: $p_\infty = 10$ bar. Initial droplet radius: $r_{d,0} = 50$ μm. Ambient temperature: (a) $T_\infty = 800$ K, (b) $T_\infty = 2000$ K.

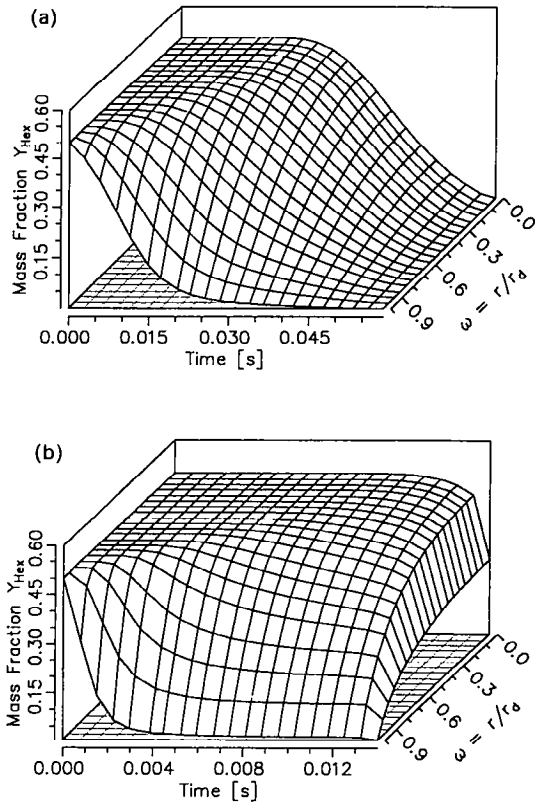

FIG. 2. Internal distribution of the more volatile component (hexane). Same conditions as in Fig. 1.

The concentration distribution of the more volatile component (hexane) is shown in Fig. 2. Here the ω and t-axes are interchanged compared to Fig. 1 for ease of representation. At high gas temperatures, the center composition ($\omega = 0$) is almost unaffected except towards the final stage of the droplet vaporization. In the first part of the droplet life the diffusion process is restricted to a small region close to the droplet surface ($\omega = 1$). At moderate gas temperatures the diffusive process already is visible at the center after one-third of the droplet lifetime. This mainly results from a decreased surface regression rate providing more time for diffusive mass transport.

The effects of diffusion controlled multicomponent evaporation compared to results of single component evaporation models are shown elsewhere (Kneer *et al.* [38]). Considering the total surface vapor mass fraction the multicomponent evaporation results have been superior to the single component models.

Variation of liquid properties

The variation of the liquid phase properties due to internal concentration and temperature gradients is depicted in Figs. 3 and 4. A complete listing of the correlations used to determine the thermophysical properties of gas and liquid phase is shown in Table 1.

For a high gas temperature, Fig. 3 shows the

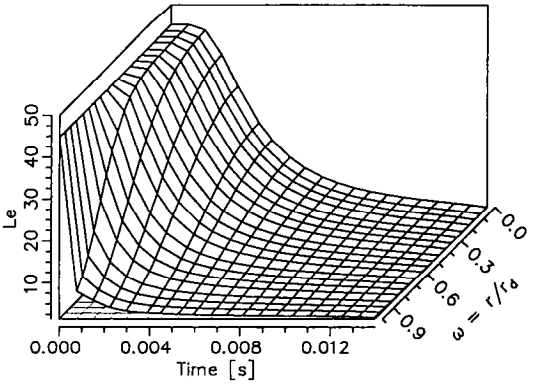

FIG. 3. Lewis number distribution for the liquid. Same conditions as in Fig. 1 ($T_\infty = 2000$ K).

behavior of the liquid phase Lewis number, $Le = Sc/Pr = \lambda/\rho c_p D$. The Lewis number describes the ratio of thermal to mass diffusion and comprises the influence of all liquid properties. Here, it decreases from the initial value of $Le \approx 50$ about one order of magnitude. These considerable changes result from the diffusion coefficient, which increases approximately by a factor of five, and from the decreasing thermal diffusivity, which is reduced to half of its

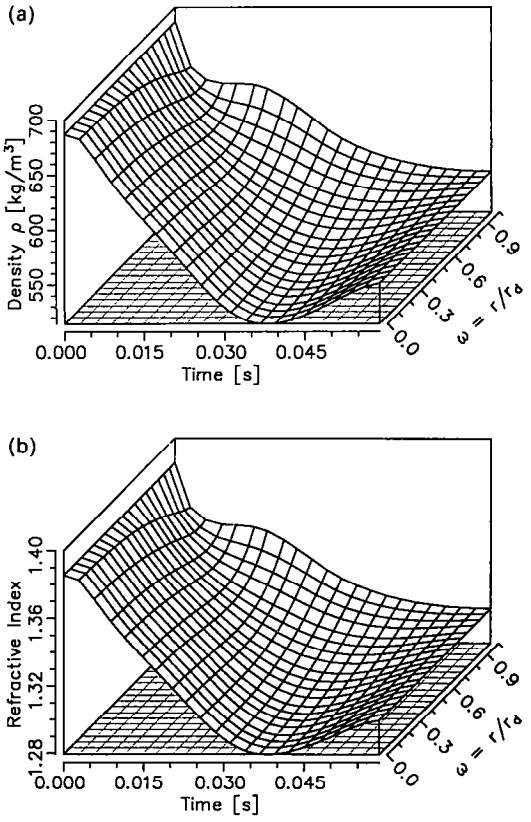

FIG. 4. Density and refractive index inside the droplet for a moderate temperature level of $T_\infty = 800$ K. Other conditions as in Fig. 1.

initial value. Both parameters are mainly controlled by the increasing droplet temperature.

A similar temporal Lewis number development can be observed for both ambient gas temperature levels. The temporal development of the internal concentration profiles, as illustrated in Figs. 2(a) and (b), implies quite different results with respect to diffusional resistance, although a similar temporal Lewis number development can be observed for both ambient gas temperature levels. This indicates that the effect of composition on the liquid thermophysical properties is of minor influence compared to the effect of temperature.

Frequently, the diffusional behavior of the liquid phase is characterized by the liquid Lewis number. However, the present results, based on variable properties, show that the Lewis number does not seem to be an appropriate parameter to assess the vaporization behavior. Thus, the description of diffusion controlled vaporization should also include the time-dependence of the diffusion process. The use of an instantaneous Peclet number, as suggested by Makino and Law [36], appears to be more suitable. This number is defined as the ratio of the surface regression rate and the diffusion coefficient ($Pe_l = K_s(t)/D_l$), comprising the influence of different gas phase conditions. Reference Peclet numbers referring to ref. [36] are determined for the present cases and are equal to $Pe_l^0 = 2.14$ and $Pe_l^0 = 7.66$, respectively, for moderate and high gas temperatures.

In contrast to the temperature-dominated variation of Lewis number, the liquid density depends on both composition and temperature development inside the droplet. The temporal and spatial variation of the liquid density is shown in Fig. 4(a) for a moderate gas temperature.

The density variations can exceed more than twenty-five percent of the initial value ($\rho_{d,0} \approx 690$ [kg m^{-3}]). The lower limit for the density is marked by the critical density of the droplet components, which has a value of $\rho_k \approx 235$ [kg m^{-3}]. Figure 4(a) shows the decrease of density due to the increasing droplet temperature, especially for the droplet center ($\omega = 0$), where the composition is unchanged in the early stage of the vaporization. At the surface of the droplet ($\omega = 1$) the density shows a slight increase after the initial sudden decrease, resulting in gradients between the center and the surface. These gradients and the increase of the center value after about half the droplet lifetime are caused by the variations in droplet composition. Here, the loss of the more volatile and lighter heptane counteracts the temperature induced decrease of density.

With respect to experimental applications the prediction of the refractive index is an additional important aspect of multicomponent droplet vaporization calculations. Based on the quasi-proportional relation between refractive index and density, refractive index changes ranging from the initial value of $n = 1.385$ down to a value of $n = 1.28$ can be observed in Fig. 4(b). A detailed description of this relation for a multicomponent liquid is given in the Appendix.

These refractive index variations may have a distinct impact on the accuracy of droplet size measurements by means of optical particle sizing techniques, e.g. phase Doppler measurements. The accuracy of the phase Doppler particle sizing technique strongly depends on the accurate knowledge of the refractive index of the droplets. In a recent study conducted by Pitcher *et al.* [50], an attempt is made to estimate the error implied by neglecting variations of the refractive index. Only temporal variations of the refractive index are considered, neglecting internal gradients. Results based on the present model including fully variable liquid properties reveal that variations of the refractive index are also likely to occur within the droplet during the vaporization process. Thus, the present study provides important data serving as a basis for the selection of appropriate refractive indices for the phase Doppler droplet sizing technique.

Comparison with constant property calculations

In demonstrating the effects of liquid property variations on the vaporization process, results from the present model are compared with results from the original constant property model. In using the constant property formulation of the Diffusion Limit Model, the thermophysical properties of the droplet components should be selected properly to balance the variations shown in Figs. 3 and 4. As commonly practiced, this balance is made by the choice of reference conditions (temperature and composition) for the determination of the thermophysical properties.

(a) *Results for liquid phase and gas phase.* The reference values for the constant property calculation are determined following Abramzon and Sirignano [24]. For example, the reference temperature is evaluated as the arithmetic mean of the initial droplet temperature and the molar-averaged boiling temperature.† In Fig. 5(a) the mass ratio of the droplet components shows large deviations of the constant property results compared to the present variable property model, especially towards the final stage of the droplet lifetime. The liquid mass ratio gives an integral information on the droplet evaporation behavior and is found to be a very sensitive quantity on the determination of the thermophysical properties, as shown later. Illustrating the effects on the gas phase, the overall vapor surface mass fraction and the mass fraction of the more volatile component are shown in Fig. 5(b) and Figs. 6(a) and (b), respectively. An immediate observation is that deviations occur mainly in the second half of the droplet lifetime. They are caused by a considerable increase of the diffusion coefficient of the liquid. Towards the final stage of the droplet life the diffusion coefficient is raised to a value

† The boiling temperature comprises the influence of the ambient pressure level.

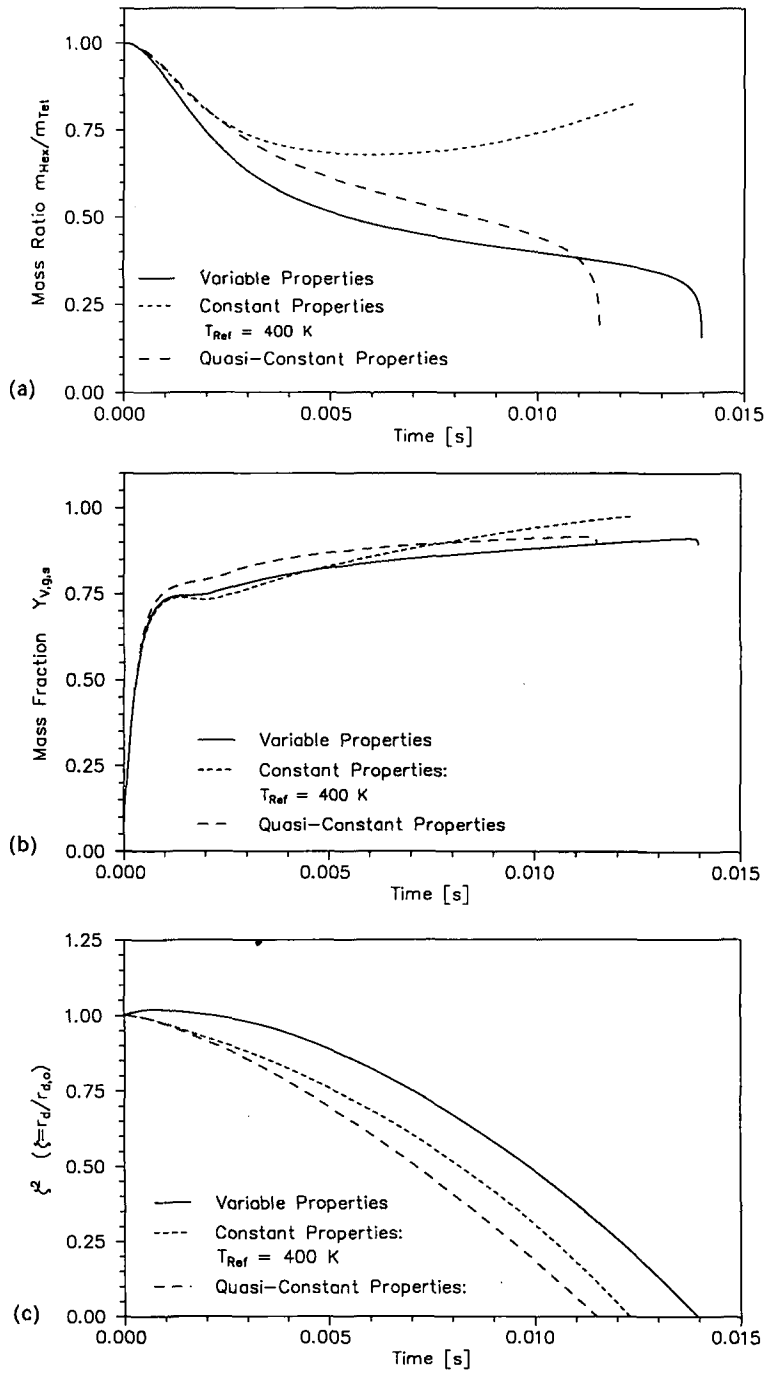

FIG. 5. Performance of different model formulations with respect to histories of liquid and vapor properties. T_∞ = 2000 K, other conditions as in Fig. 1. (a) Liquid mass ratio. (b) Total vapor mass fraction at droplet surface. (c) Non-dimensional diameter squared.

about five-times as high as the initial value, with the diffusional resistance decreasing markedly. Thus, in the variable property case this leads to a reduced liquid mass fraction and to a lower surface vapor mass fraction of the more volatile component.

It should be noted that the liquid thermal diffusivity also varies. In contrast to the diffusion coefficient, however, it decreases only to half of its initial value. Variations of the thermal diffusivity, though, appear to become less significant, since the heat flux at the droplet surface decreases rapidly during the vaporization.

(b) *Quasi-constant property calculation.* The governing equations, (9) and (10), have been analyzed with regard to the additional terms resulting from variable property formulation. In particular, these are the local

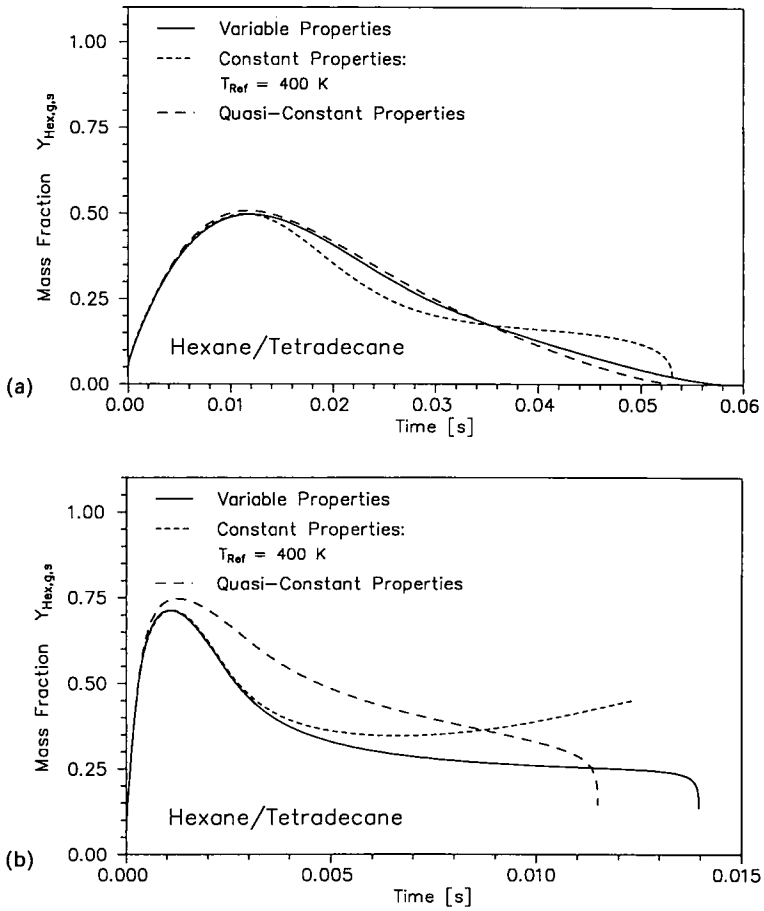

FIG. 6. Temporal change of surface mass fraction of the more volatile component (hexane). Same conditions as in Fig. 1.

derivative of thermal conductivity, in the energy equation, (9), and the local derivatives of density and diffusion coefficient as well as the time derivative of density,† in the species equation, (10). The time derivative of the dimensionless radius employed in equations (9) and (10) is also a function of density, which can be seen in equation (11).

A detailed analysis of these terms led to the following conclusions:

The local derivatives of the diffusion coefficient and the density are small compared to the remaining terms, except at the droplet surface. These derivatives have different signs and, therefore, tend to cancel each other. Additionally, these terms are of minor influence regarding the fact that the second derivative of the main variable (i.e. concentration) is considerably larger than its first derivative. The latter fact also applies for the energy equation, where the local derivative of the thermal conductivity is of negligible influence.

A more relevant term is the time derivative of the density. This term is relatively large in the early stage of the vaporization process, where it reaches its maximum at the droplet surface. This is due to the rapid heating up of the droplet surface, causing large internal temperature gradients. The increased surface temperature determines the decrease of the density and thus controls the droplet diameter rise (see Fig. 5(c)). Neglecting the variation of liquid density mostly leads to errors in the determination of the droplet diameter, see equation (11). It is important to consider this term for comparisons of results from particle sizing methods in hot combustor flows and theoretical calculations.

Examining the influence of the property changes, a calculation has been performed neglecting all the terms described above. In contrast to a constant property formulation, the liquid thermophysical properties are updated after each timestep executed (quasi-constant property formulation). For moderate gas temperatures only minor deviations occur compared to results from variable property calculations (Fig. 6(a)). For high gas temperatures (Fig. 6(b)) deviations are more pronounced due to larger spatial and, in particular, temporal temperature gradients causing larger

† Last line of equation (10). The spatial derivative in the last term is due to nondimensionalization.

property gradients. It is found that the accuracy of the quasi-constant property formulation is similar to the one of the constant property formulation, when both formulations are compared to results of the fully variable property model. Since the variable and quasi-constant property model require approximately the same amount of computing time and therefore represent rather time-consuming droplet models, it seems reasonable to improve the constant property model utilizing results from the variable property model. This is important especially for a comprehensive spray analysis where only a certain degree of complexity of the droplet model used is possible.

(c) *Reference values for constant property calcu-*

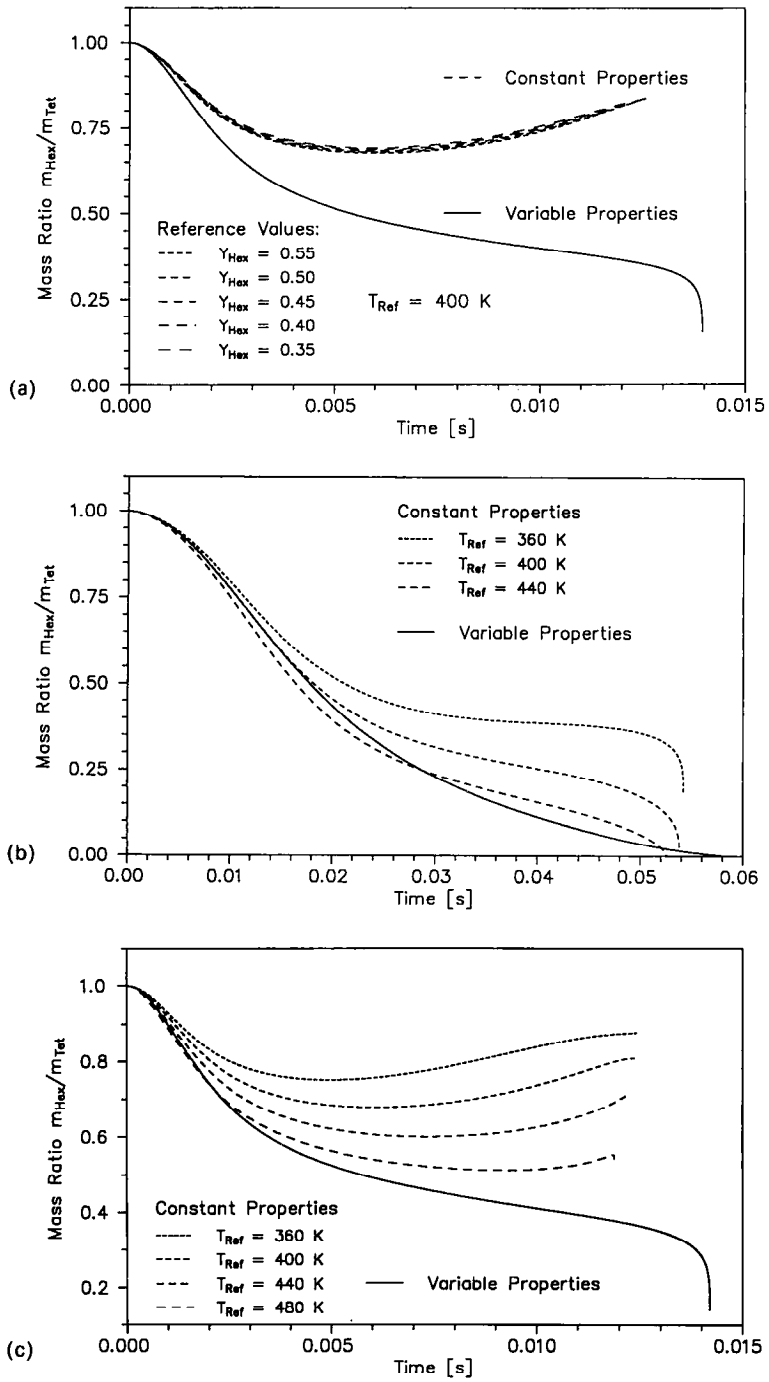

FIG. 7. Influence of reference values on the results of the constant property formulation. Same conditions as in Fig. 1. (a) Constant liquid reference temperature: T_{ref} = 400 K. Ambient temperature: T_∞ = 2000 K. (b) and (c) Constant liquid reference composition: Y_{Hex} = 0.5. Ambient temperature: (b) T_∞ = 800 K. (c) T_∞ = 2000 K.

lations. Constant property calculations require the use of averaged thermophysical property values. These are determined at the same temperature and concentration levels, the so-called reference values. Results from the variable property model serve as a measure to compare with those from constant property calculation. As demonstrated above, the liquid mass ratio is again chosen as indicator.

In Fig. 7(a) results based on the constant property formulation are shown for various reference droplet compositions selected within a reasonable range. It can be observed that the influence of concentrations on the liquid mass ratio is small. Figures 7(b) and (c) show results for various reference temperatures. In this case, there is a considerable effect on the deviation from the more accurate variable property calculation.

Therefore, the reference temperature for constant property calculations has to be selected carefully. Additional calculations have shown that the optimization of the reference temperature should be conducted with regard to the gas temperature. Higher gas temperatures will lead to higher droplet temperatures towards the final stage of droplet vaporization and, therefore, the reference temperature needs to be increased. It is suggested to modify the criterion of Abramzon and Sirignano [24] as follows

$$T_{\mathrm{ref}} = A(T_\infty)(T_0 + T_{\mathrm{boil}}) \tag{15}$$

where

$$A(T_\infty) = 0.55 \div 0.6. \tag{16}$$

The lower limit represents the moderate gas temperature case and the higher limit the high gas temperature case. The corresponding values of the reference temperature are $T_{\mathrm{ref}} = 440$ K and $T_{\mathrm{ref}} = 480$ K, compared to a value of $T_{\mathrm{ref}} = 400$ K obtained with the original criterion. The reference composition can be equal to the initial composition due to its minor influence.

The present criterion implies basically two modifications compared to the proposal of Abramzon and Sirignano. First, the reference temperature is dependent also on the gas temperature, determining the droplet internal temperature history. Secondly, the reference temperature is higher leading to a higher diffusion coefficient and thus attaining better results with regard to the variable property model. The improvement concerns mainly the second half of the droplet lifetime, where the deviations are largest. However, about 50% of the droplet mass still will evaporate in this phase of the droplet lifetime.

The effects described above also apply for the forced convective heat transfer at the droplet surface, as shown in Fig. 8. The droplet (initial velocity $u_{d,0} = 1$ m s^{-1}) is moving in a one-dimensional gas environment, which is at a constant speed of $u_\infty = 20$ m s^{-1}. The main difference in the droplet life history is given by the different time scaling compared to the stagnant droplet case. Here, the major changes of most of the important quantities take place in the early stage of the droplet life time. The reason is the enhanced mass transfer due to the forced convection. A comparison of Figs. 7(b) and 8 shows that convection tends to result in larger deviations of the constant property formulation compared to the variable property solution.

In the present paper, empirical correlations (see Table 1) developed for conditions far away from the critical state are used for the evaluation of thermophysical properties. Therefore, the high droplet temperatures towards the final stage of the droplet's lifetime will cause some uncertainties in the vapor–liquid equilibrium conditions at the droplet surface (cf. heat of vaporization). These shortcomings are a common feature of all the multicomponent droplet vaporization models developed up to now and may be avoided with a consistent thermodynamical formulation (cf. Hsieh *et al.* [51]). This equation of state

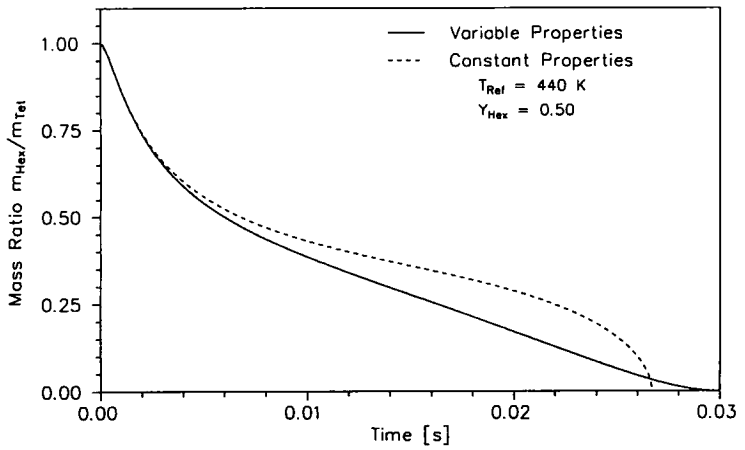

FIG. 8. Reference value influence in the convective case ($u_{d,0} = 1$ m s^{-1}, $u_\infty = 20$ m s^{-1}). Same conditions as in Fig. 1.

approach considerably increases the computational effort.

CONCLUSIONS

The present study is concerned with the variation of liquid properties occuring during the vaporization of multicomponent droplets. An extended Diffusion Limit Model accounting for variable properties has been developed and tested for an isolated droplet under moderate and high gas temperature conditions. Pronounced variations of the liquid properties during the vaporization process act to lower the diffusional resistance within the droplet mainly in the second half of the droplet lifetime. The characterization of the vaporization behavior with regard to liquid diffusion using the Lewis number fails due to non-consideration of the ambient conditions. Internal temperature and concentration gradients also lead to considerable variations of the liquid density and the refractive index as the vaporization proceeds. These results can serve to improve the error prediction in optical diagnostics such as in phase Doppler particle sizing techniques.

The governing equations of the modified model have been analyzed with respect to the influence of the liquid properties. For moderate temperatures it seems possible to use a quasi-constant property formulation. However, both (the fully variable property model and the quasi-constant property formulation) are found to be rather time-consuming models.

A comparison of results from constant property calculations with those employing variable properties shows remarkable deviations depending on the selection of the reference values for the constant properties. Therefore, it seems most promising to use the variable property model as a measure to determine appropriate reference values. Thus, an improved criterion to determine reference values is given. This new criterion even allows the calculation of multicomponent spray evaporation, which requires the use of the less time-consuming constant property formulation.

Acknowledgement—The present study was supported by a grant from the SFB 167 (high intensity combustors) of the Deutsche Forschungsgemeinschaft.

REFERENCES

1. S. Wittig, W. Klausmann and B. Noll, Turbulence effects on the droplet distribution behind airblast atomizers, AGARD-CP-422, *Combustion and Fuels in Gas Turbine Engines*, p. 5 (1987).
2. S. Wittig, W. Klausmann, B. Noll and J. Himmelsbach, Evaporation of fuel droplets in turbulent combustor flow, ASME-88-GT-107, *Presented at the Gas Turbine and Aeroengine Congress Amsterdam*, The Netherlands, 6–9 June (1988).
3. R. B. Landis and A. F. Mills, Effect of internal diffusional resistance on the evaporation of binary droplets, *Proc. 5th Int. Heat Transfer Conf. Tokyo Section* **B7.9,** 345–349 (1974).
4. C. K. Law, Internal boiling and superheating in vaporizing multicomponent droplets, *A.I.Ch.E. Jl* **24,** 626–632 (1978).
5. W. A. Sirignano, Fuel droplet vaporization and spray combustion theory, *Prog. Energy Combust. Sci.* **9,** 291–332 (1983).
6. W. A. Sirignano, An integrated approach to spray combustion model development, *Combust. Sci. Tech.* **58,** 231–251 (1988).
7. G. M. Faeth, Current status of droplet and liquid combustion, *Prog. Energy Combust. Sci.* **3,** 191–224 (1977).
8. C. K. Law, Recent advances in droplet vaporization and combustion, *Prog. Energy Combust. Sci.* **8,** 171–201 (1982).
9. H. A. Dwyer and B. R. Sanders, Detailed computation of unsteady droplet dynamics, *Proc. 20th Symposium (Int.) Combustion/The Combustion Institute* 1743–1749 (1984).
10. B. R. Sanders and H. A. Dwyer, Modeling unsteady droplet combustion processes, *Proc. 2nd ASME–JSME Thermal Engng Joint Conf.*, Honolulu, Hawaii, Vol. 1, 3–10 (1987).
11. R. Haywood, R. Nafziger and M. Renksizbulut, A detailed examination of gas and liquid phase transient processes in convective droplet evaporation, *J. Heat Transfer* **111,** 495–502 (1989).
12. R. Haywood and M. Renksizbulut, On variable-property, blowing, and transient effects in convective droplet evaporation with internal circulation, *Proc. 8th Int. Heat Transfer Conf.*, San Francisco, 1861–1866 (1986).
13. D. L. R. Oliver and J. N. Chung, Unsteady conjugate heat transfer from a translating fluid sphere at moderate Reynolds numbers liquid droplet: solutions for intermediate Reynolds numbers, *Int. J. Heat Mass Transfer* **33,** 401–408 (1990).
14. L. J. Huang and P. S. Ayyaswamy, Evaporation of a moving liquid droplet: solutions for intermediate Reynolds numbers, *Natl Heat Transfer Conf.*, HDT-Vol. 106, 431–437 (1989).
15. S. S. Sadhal and P. S. Ayyaswamy, Flow past a liquid drop with a large non-uniform radial velocity, *J. Fluid Mech.* **133,** 65–81 (1983).
16. M. Renksizbulut and M. C. Yuen, Numerical study of droplet evaporation in a high-temperature stream, *J. Heat Transfer* **105,** 389–397 (1983).
17. M. Renksizbulut and R. J. Haywood, Transient droplet evaporation with variable properties and internal circulation at intermediate Reynolds numbers, *Int. J. Multiphase Flow* **14,** 189–202 (1988).
18. Q.-V. Nguyen, R. H. Rangel and D. Dunn-Rankin, Measurement and prediction of trajectories and collision of droplets, *Int. J. Multiphase Flow* **17,** 159–177 (1991).
19. S. Prakash and W. A. Sirignano, Liquid fuel droplet heating with internal circulation, *Int. J. Heat Mass Transfer* **21,** 885–895 (1978).
20. S. Prakash and W. A. Sirignano, Theory of convective fuel droplet vaporization with unsteady heat transfer in the circulating liquid phase, *Int. J. Heat Mass Transfer* **23,** 253–268 (1980).
21. M. J. M. Hill, On a spherical vortex, *Phil. Trans. Roy. Soc. Lond. A* **185,** 213–245 (1894).
22. P. Lara-Urbaneja and W. A. Sirignano, Theory of transient multicomponent droplet vaporization in a convective field, *Proc. 18th Symposium (Int.) Combustion/The Combustion Institute*, 1365–1374 (1981).
23. A. Y. Tong and W. A. Sirignano, Multicomponent droplet vaporization in high temperature gas, *Combust. Flame* **66,** 221–235 (1986).
24. B. Abramzon and W. A. Sirignano, Approximate theory of a single droplet vaporization in a convective field: effects of variable properties, Stefan flow and transient liquid heating, *Proc. 2nd ASME–JSME Thermal Engng Joint Conf.*, Honolulu, Hawaii, Vol. 1, 11–18 (1987).
25. D. G. Talley and S. C. Yao, A semi-empirical approach to thermal and composition transients inside vaporizing fuel droplets, *Proc. 21st Symposium (Int.) Combustion/The Combustion Institute*, 609–616 (1986).

26. S. K. Aggarwal, Modeling of a dilute vaporizing multicomponent fuel spray, *Int. J. Heat Mass Transfer* **30,** 1949–1961 (1987).
27. S. K. Aggarwal, Further results on evaporating bicomponent fuel sprays, *Int. J. Heat Mass Transfer* **31,** 2593–2597 (1988).
28. J. E. D. Gauthier, M. F. Bardon and V. K. Rao, Combustion characteristics of multicomponent fuels under cold starting conditions in a gas turbine, *Presented at the International Gas Turbine and Aeroengine Congress and Exposition*, Orlando, FL, 3–6 June, ASME 91-GT-109 (1991).
29. C. A. Bergeron and W. L. H. Hallett, Autoignition of single droplets of two-component liquid fuels, *Combust. Sci. Tech.* **65,** 181–194 (1989).
30. C. Presser, H. G. Semerjan, A. K. Gupta and C. T. Avedisian, Combustion of methanol and methanol/dodecanol spray flames, *AIAA/SAE/ASME/ASEE 26th Joint Propulsion Conf.*, Orlando, FL, 16–18 July, AIAA 90-2446 (1990).
31. J. C. Lasheras, L. T. Yap and F. L. Dryer, Effect of the ambient pressure on the explosive burning of emulsified and multicomponent fuel droplets, *Proc. 20th Symposium (Int.) Combustion/The Combustion Institute*, 1761–1772 (1984).
32. C. H. Wang, X. Q. Liu and C. K. Law, Combustion and microexplosion of freely falling multicomponent droplets, *Combust. Flame* **56,** 175–197 (1984).
33. G. L. Hubbard, V. E. Denny and A. F. Mills, Droplet evaporation: effects of transients and variable properties, *Int. J. Heat Mass Transfer* **18,** 1003–1008 (1975).
34. B. Abramzon and W. A. Sirignano, Droplet vaporization model for spray combustion calculations, *Int. J. Heat Mass Transfer* **32,** 1605–1618 (1989).
35. N. Frössling, Über die Verdunstung fallender Tropfen, *Gerlands Beiträge zur Geophysik* **52,** 171–216 (1938).
36. A. Makino and C. K. Law, On the controlling parameter in the gasification behavior of multicomponent droplets, *Combust. Flame* **73,** 331–336 (1988).
37. A. C. Hindmarsh, ODEPACK, a systemized collection of ODE solvers. In *Scientific Computing* (Edited by R. S. Stepleman *et al.*), p. 55. North-Holland, Amsterdam (1983).
38. R. Kneer, M. Schneider, B. Noll and S. Wittig, Effects of variable liquid properties on multicomponent droplet vaporization, ASME-92-GT-131, Presented at the Gas Turbine and Aeroengine Congress Cologne, Germany, June 1–4 (1992).
39. R. C. Reid, J. M. Prausnitz and T. K. Sherwood, *The Properties of Gases and Liquids* (3rd Edn). McGraw-Hill, New York (1977).
40. C. F. Spencer and R. P. Danner, Prediction of bubble-point density of mixtures, *J. Chem. Engng Data* **18,** 230–234 (1973).
41. C. F. Spencer and S. B. Adler, A critical review of equations for predicting saturated liquid density, *J. Chem. Engng Data* **23,** 82–89 (1978).
42. T. E. Daubert, American Petroleum Institute, *Technical Data Book—Petroleum Refining, metric edition*, Am. Petrol. Institute, Washington, DC (1985).
43. K. M. Watson and E. F. Nelson, Improved methods for approximating critical and thermal properties of petroleum fractions, *Ind. Engng Chem.* **25,** 880–887 (1933).
44. R. C. Reid, J. M. Prausnitz and B. E. Poling, *The Properties of Gases and Liquids* (4th Edn). McGraw-Hill, New York (1986).
45. B. I. Lee and M. G. Kesler, A generalized thermodynamic correlation on three-parameter corresponding states, *A.I.Ch.E. Jl* **21,** 510–527 (1975).
46. K. Lucas, Berechnungsmethoden für Stoffeigenschaften. In *VDI- Wärmeatlas*, Kap. Da (1984).
47. R. B. Bird, W. E. Stewart and E. N. Lightfoot, *Transport Phenomena*. J. Wiley & Sons, New York (1960).
48. K. M. Watson, Thermodynamics of the liquid state: generalized prediction of properties, *Ind. Engng Chem.* **35,** 398–406 (1943).
49. N. B. Vargaftik, *Handbook of Physical Properties of Liquids and Gases* (2nd Edn). Hemisphere, Washington (1975).
50. G. Pitcher, G. Wigley and M. Saffman, Sensitivity of dropsize measurements by phase Doppler anemometry to refractive index changes in combusting fuel sprays, *Proc. 5th Int. Symp. Appl. Laser Techn. Fluid Mech.*, 9–12 July, Lisbon, Portugal, paper 14.4 (1990).
51. K. C. Hsieh, J. S. Shuen and V. Yang, Droplet vaporization in high-pressure environments I: near critical conditions, *Combust.Sci. Tech.* **76,** 111–132 (1991).
52. P. W. Atkins, *Physical Chemistry* (4th Edn). Oxford University Press, Oxford (1990).
53. M. Born, *Optik*. Springer, Berlin (1972).

APPENDIX

Temperature and concentration variation of the refractive index† (see Atkins [52] and Born [53]):

The polarizability of a liquid or gaseous medium exposed to an electromagnetic field at high frequencies, e.g. the frequency spectrum of the visible light, represents an atomic constant depending only on the specified frequency (Lorentz–Lorentz law). Expressed in terms of molar refractivity the Lorentz–Lorentz law is given by

$$R_m = \frac{M}{\rho}\frac{n^2-1}{n^2+2} \tag{17}$$

where R_m depends only on the light frequency ν. If equation (17) is applied to mixtures the molar refractivity can be expressed as

$$R_m = X_1 R_{m1} + X_2 R_{m2} + \cdots. \tag{18}$$

In the case of a medium with variable thermophysical properties, for example an evaporating binary liquid, the refractive index can be obtained applying the following three step scheme:

(i) Calculation of constants:

based on the known values of the single component refractive indices $n_i(\nu, T_0)$‡ and densities $\rho_i(T_0)$§ at temperature T_0 the constant molar refractivities of the components are given by

$$R_{mi}(\nu) = \frac{M_i}{\rho_i(T_0)}\frac{n_i^2(\nu, T_0)-1}{n_i^2(\nu, T_0)+2}. \tag{19}$$

(ii) Determination of the mixture molar refractivity ($R_m(\nu)$) by application of equations (19) and (18).

(iii) Refractive index of the mixture, derived from equation (18)

$$n^2(\nu, T) = \frac{V_m(T)+2R_m(\nu)}{V_m(T)-R_m(\nu)} \tag{20}$$

where $V_m = (M/\rho_d(T))$ is the molar volume of the mixture.

If temperature and composition within a multicomponent droplet are known, that is the distribution of $\rho_d(T)$, equation (20) yields the corresponding distribution of the refractive index.

† The refractive index is a complex quantity, but with respect to PDA measurements only the real part is of interest.

‡ Here: sodium D-line (λ = 589 nm).

§ Based on: Daubert, T.E.: API-Technical Data Book, metric edition [42].